

1 Individual alpha power predicts language comprehension

2

3 P. Wang¹, Y. He³, B. Maess¹, J. Yue⁵, L. Chen^{2,6}, J. Brauer^{2,4}, A.D. Friederici², T.R. Knösche^{1*}

4

5 ¹ Max Planck Institute for Human Cognitive and Brain Sciences, Brain Networks Group, Leipzig,
6 Germany

7 ² Max Planck Institute for Human Cognitive and Brain Sciences, Department of Neuropsychology,
8 Leipzig, Germany

9 ³ Philipps University Marburg, Department of Psychiatry and Psychotherapy, Marburg, Germany

10 ⁴ Friedrich Schiller University, Office of the Vice-President for Young Researchers, Jena, Germany

11 ⁵ Harbin Institute of Technology, Laboratory for Cognitive and Social Neuroscience, School of
12 Management, Harbin, China

13 ⁶ Beijing Normal University, College of Chinese Language and Culture, Beijing, China

14

15 Keywords

16 Individual alpha, alpha attenuation, EEG/MEG, sentence comprehension, embedded sentences

17

18 Highlights

19

20 ● Comprehension of structurally complexed embedded sentences is correlated with individual alpha
21 power attenuation during task but not with alpha power at rest.

22 ● These effects were localized in temporal-parietal brain regions known to be associated with
23 language processing.

24

25 Data availability statement

26 Anonymized raw data will be made available upon request via email to the corresponding author
27 provided the requesting researchers sign a formal data sharing agreement and cite this paper as origin
28 of the data.

29

30

31 Corresponding author:

32 Thomas R. Knösche (knoesche@cbs.mpg.de)

33 **Abstract**

34

35 Alpha power attenuation during cognitive task performing has been suggested
36 to reflect a process of release of inhibition, increase of excitability, and thereby
37 benefit the improvement of performance. Here, we hypothesized that changes in
38 individual alpha power during the execution of a complex language comprehension
39 task may correlate with the individual performance in that task. We tested this using
40 magnetoencephalography (MEG) recorded during comprehension of German
41 sentences of different syntactic complexity.

42 Results showed that neither the frequency nor the power of the spontaneous
43 oscillatory activity at rest were associated with the individual performance. However,
44 during the execution of a sentences processing task, the individual alpha power
45 attenuation did correlate with individual language comprehension performance.
46 Source reconstruction localized effects in temporal-parietal regions of both
47 hemispheres. While the effect of increased task difficulty is localized in the right
48 hemisphere, the difference in power attenuation between tasks of different complexity
49 exhibiting a correlation with performance was localized in left temporal-parietal brain
50 regions known to be associated with language processing.

51 From our results, we conclude that in-task attenuation of individual alpha
52 power is related to the essential mechanisms of the underlying cognitive processes,
53 rather than merely to general phenomena like attention or vigilance.

54 **1. Introduction**

55

56 The alpha band (8-12 Hz) typically forms the most stable and prominent peak
57 in the EEG/MEG power spectrum (Berger, 1938; Schomer & Da Silva, 2012). These
58 oscillations evidently play a major role in brain function at rest, as their power is
59 attenuated in the task-relevant brain regions during various movement or cognitive
60 tasks, including finger tapping, driving, arithmetic calculations, and sentence
61 comprehension (Gastaldon et al., 2020; Klimesch et al., 1990; Magosso et al., 2019;
62 Mann et al., 1996; Pfurtscheller, 1989; Wang et al., 2021). The power attenuation in
63 the alpha band has also been shown to scale with task demand or engagement at the
64 group level (Magosso et al., 2019; Wang et al., 2021). This phenomenon has been
65 associated with cortical activation or release from inhibition due to the task (Klimesch,
66 2012; Pfurtscheller, 2003). It has also been shown, at the individual level, that the
67 alpha power at rest or immediately before the task correlates with task performance
68 (Jones et al., 2010; Van Dijk et al., 2008; van Ede et al., 2012), but evidence for such
69 an individual relationship for the task-related power attenuation during task
70 performance is scarce (Hilla et al., 2020). Therefore, the question remains whether the
71 attenuation phenomenon is related to the essential mechanisms of the underlying
72 cognitive processes, rather than merely to general phenomena like attention or
73 vigilance.

74 Moreover, the characteristics of the alpha peak (e.g., frequency and power) are
75 specific for each individual (Furman et al., 2018; Grabot & Kayser, 2020; Gulbinaite
76 et al., 2017; Horschig et al., 2014; Katyal et al., 2019; Migliorati et al., 2020; Minami
77 et al., 2020; Sadaghiani & Kleinschmidt, 2016; Smit et al., 2006). Hence, the
78 somewhat non-univocal picture on the relationship between individual alpha power
79 dynamics and task performance might also be rooted in the insufficient capture of the
80 individual oscillations by using the classical broad frequency band (about 8-12 Hz).

81 In order to clarify the question if the individual alpha power attenuation is
82 related to cognitive performance, we turn to the arguably most 'human-like' cognitive
83 faculty, namely language. The ability to produce and understand language requires
84 intense coordination of numerous cognition faculties, such as phonological perception,
85 syntax processing, semantic association, working memory, attention, and motor
86 control. Indeed, it has been shown that the individual alpha peak frequency as well as

87 the alpha band power at rest are related to individual language abilities (Kwok et al.,
88 2019; Rathee et al., 2020; Sklar et al., 1972). Recently, we have explored the alpha
89 band power directly *during* a language task, and found an association between the
90 alpha power attenuation and language task complexity (Wang et al., 2021).
91 Consequently, we hypothesize that the difference in alpha power attenuation between
92 language tasks of different complexity, gauged at the individual alpha peak frequency
93 and in task-relevant brain regions, reflects the individual cognitive ability to handle
94 the task, and hence might be associated with the observed performance.

95 In the present paper, we tested this hypothesis using the same data set as in our
96 previously reported MEG study with healthy, native German adult speakers (Wang et
97 al., 2021). On four days within a week, participants listened to complex German
98 sentences, and answered probing questions regarding the thematic role assignment
99 (“who is doing what to whom”). The sentences differed in their complexity by
100 containing either single or double embedded relative clauses. Previously, we reported
101 that the cortical (posterior superior temporal and adjacent parietal) alpha band power
102 attenuation at the final embedding closure was significantly larger for double than for
103 single embedded sentences (Wang et al., 2021). Here, rather than looking at the entire
104 alpha band, we focus on the individual peak frequency obtained from the resting state.
105 In particular, we examined the correlation between language performance and: (1) the
106 individual peak frequency and its power at rest; (2) the power attenuation of the
107 individual peak frequency during the experimental task at different syntactic positions
108 in the sentences; (3) the spatial localization on the cortex for the observed correlation
109 effects. The results confirm our hypothesis that the individual difference between the
110 power attenuation for tasks of different complexities (double vs. single embedding
111 sentence comprehension) correlates with the individual performance.

112

113 **2. Materials and Methods**

114 As we are reusing the data from our previous study, many of the
115 methodological details are already described elsewhere (Wang et al., 2021). In the
116 following, these aspects are just presented as brief summary.

117 **2.1. Participants**

118 Thirty right-handed native German speakers (fifteen females) were enrolled in
119 this study (mean age: 27, range from 20 to 34). Their reading span was 3.7 ± 0.9
120 (mean \pm SD). No neurological diseases or hearing impairments were reported.
121 Participants were naïve to the purposes of the experiment and gave written informed
122 consent prior to the experiment. The study was approved by the ethics committee of
123 the University of Leipzig (number of this approval).

124 **2.2. Stimulus material**

125 Two types of German sentences with single and double hierarchical center
126 embedding were presented (see Fig. S5). All sentences started with an introductory
127 phrase followed by a relative clause initiated by a relative pronoun (e.g. *dass / that*).
128 The beginning of each relative clause (brace) was labeled with *bxon* while the final
129 verb of it was labeled with *bxoff* to indentify the same level of embedding. The place
130 holder x represents the embedding level.

131 **2.3. Experimental procedures**

132 The experiment included four sessions carried out on four working days within
133 one week. The stimuli were presented by the software ‘Presentation’
134 (www.neurobs.com). At each day, participants listened to 33 sentences of each
135 sentence type (i.e. single and double embedded). Each participant received an
136 individual randomization of all 264 sentences presented on the four days. None of the
137 sentences was presented twice to the same participant. After each sentence, a content
138 question was asked to test the understanding of the thematic role assignments. Each
139 session comprised four blocks. Sentences were presented during the first three blocks.
140 During the fourth block, resting-state was recorded for at least 10 minutes.
141 Participants were asked to close their eyes and stay awake.

142 **2.4. Behavioral data analysis**

143 Behavioral performance was measured through the accuracy of the
144 participants’ responses to the question task. In contrast to our previous study, the
145 single valued total performance accuracy of each participant was estimated by a
146 simple mean across the 4 experimental days.

147 **2.5. MEG data acquisition and preprocessing**

148 After preprocessing, the data of the first three blocks (task sections) were
149 epoched of 0.5 s length starting with the event triggers at *b1on*, *b1off*, *b2on*, *b2off*,
150 *b3on*, and *b3off* (on for embedding's begin, and off for embedding's closure). Data of
151 the fourth block (rest section, total 12min) were epoched into 36 trials of 20s length
152 each to get a frequency resolution of 0.05 Hz for the determination of the peak
153 frequency. After artifact rejection, the median value of number of valid trials was 34,
154 ranging from a minimum of 6 to a maximum of 35.

155 **2.6. Estimation of individual spontaneous peak frequency in sensor 156 space**

157 The individual spontaneous peak frequencies were estimated from the pre-
158 processed resting-state MEG recordings. For each subject on each day, the power
159 spectrum density (PSD) for each sensor was estimated using the multi-taper method
160 via the function *psd_multitaper* from the MNE-python v.0.16 (Gramfort et al., 2013)
161 (using default setup, except normalization = 'full'). The PSDs for each 20s-length
162 trial were transformed to logarithmic scale (i.e., in dB) and then averaged cross trials
163 and sensors. After the averaging, the 1/f pink noise background was estimated and
164 subtracted from each average grand PSD. The maximal peaks between 7-29 Hz were
165 identified as the individual peak frequency.

166 **2.7. Estimation of individual peak frequency power during the task 167 in source space**

168 For source localization, we used individual single shell volume conductor
169 models and source models constructed from the individual T1-weighted MR data. We
170 utilized Freesurfer 6.0.0 to segment the inner skull as well as the cortical surface.
171 Finally, the cortical surfaces were labeled according to Glasser et al. (2016). In this
172 paper, we focused on the regions of interest (ROI), which showed significant alpha
173 power difference for different sentence type at final closure of the embeddings (*b1off*),
174 see Fig. 3A and Wang et al. (2021).

175 To estimate the alpha power in source space, we used the LCMV beamformer
176 method (Van Veen et al., 1997) via the function *make_lcmv* by MNE-python v.0.16.
177 The reconstructed current density was restricted to being perpendicular to the cortical

178 surface. The noise covariance matrix was computed by the mean noise covariance
179 from the empty room measurements obtained before and after each recording session.
180 A data covariance matrix was computed separately for each day based on the whole
181 sentence data. The PSD (in dB) of each source was estimated using the multi-taper
182 method (*psd_multitaper*, data zero-padding to 2 s), separately for each subject, ROI,
183 sentence type, and day as mean over all presented sentences. The 1/f pink noise
184 background was estimated and subtracted from each average PSD separately. To
185 estimate the spectral power of the individual peak frequency at task, we averaged the
186 spectral power of the two frequency bins, which define the interval around the
187 individual peak frequency at rest. Finally, relative power attenuation was calculated
188 by normalizing to the respective *blon* power value separately for each subject, ROI,
189 sentence type, and day. Hence, all subsequently reported spectral power values in task
190 conditions are relative power attenuations with respect to *blon*.

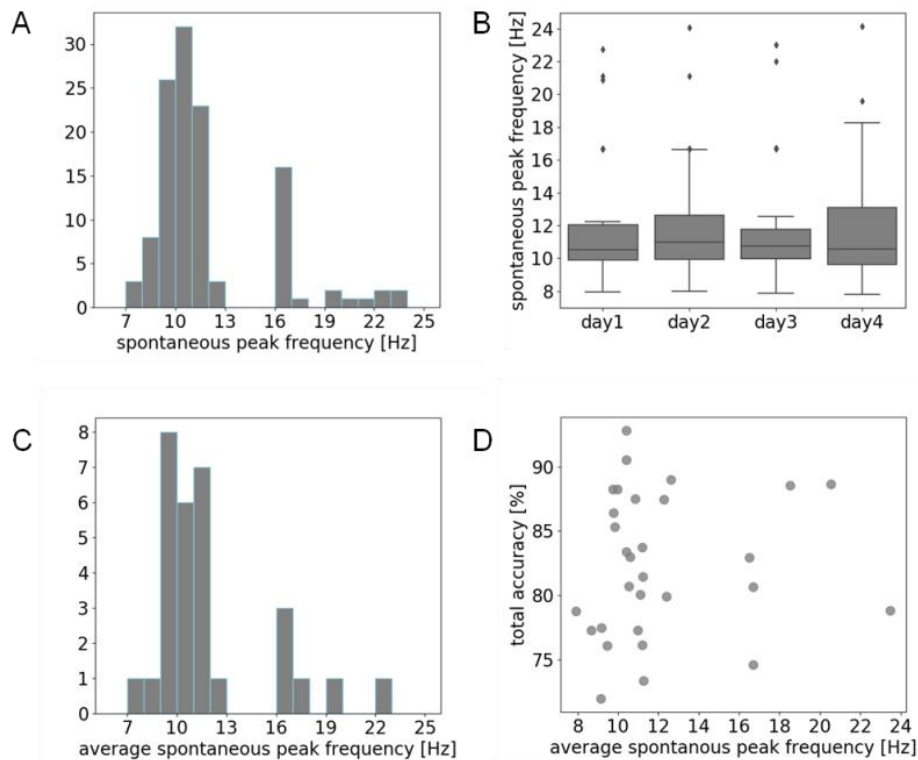
191 For computing the individual frequency power in Yeo's 17-networks (Yeo et
192 al., 2011; Fig. 5A), we first morphed the individual source space to the fsaverage
193 space via the source morph function in MNE-python v.0.16 (by setting fsaverage
194 spacing „ico5“). The remaining steps were as same as for using the Glasser's ROIs.
195

196 **3. Results**

197 *3.1. The individual resting-state peak frequency is not correlated with the language* 198 *performance*

199 We first examined the relationship between the individual peak frequency
200 during rest (averaged across four days) and the total performance accuracy. The
201 individual peak frequency was estimated from the resting-state recordings at sensor
202 level (for more details, see Materials and Methods section 2.6.). We first estimated it
203 for each subject on each day (Fig. 1A) and then averaged it across the four days (Fig.
204 1C). The overall task performance was calculated for each subject by averaging the
205 accuracy scores of the four experimental days, including, both, double and single
206 embedded sentences. As expected, for most participants, their individual peak
207 frequencies were located in the alpha frequency range (8-12 Hz; Fig. 1A,C). There
208 were 6 participants, though, whose peak frequencies were estimated in the beta range
209 (> 16 Hz). We found no statistical difference among the estimated individual peak

210 frequencies of the four experimental days (Friedman's test $Q = 0.71$, $p = 0.87$; Fig.
211 1B). We also found no clear association between the 4-day-average individual peak
212 frequency and the total performance accuracy (Spearman's correlation, $r = 0.20$, $p =$
213 0.29 ; Fig. 1D).

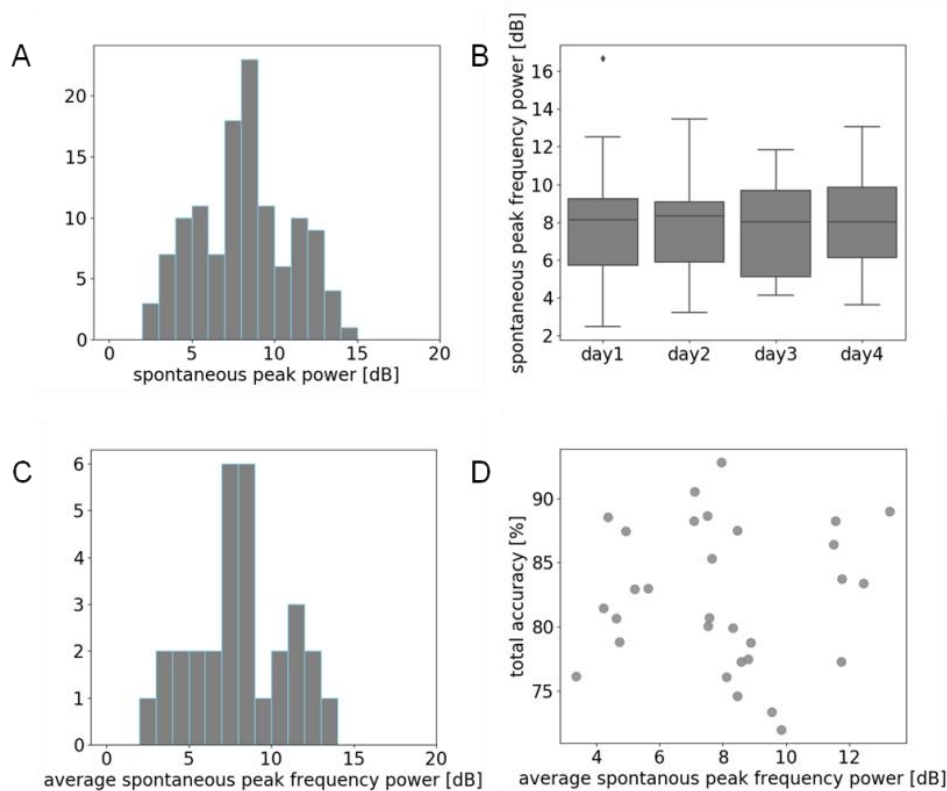


214
215 Figure 1. Relationship between the individual spontaneous peak frequency and the
216 language task performance. (A) Histogram of the 120 spontaneous peak frequencies
217 of the thirty participants on all four experimental days. (B) Boxplot of the participants'
218 individual spontaneous peak frequencies on each training day. The boxes show the
219 interquartile ranges that stretch from the first quartile (25th percentile) to the third
220 quartile (75th percentile) with the black line marking the median (50th percentile). The
221 maximal whisker range is 1.5 times the interquartile range. Note that the displayed
222 whisker length depends on values within whisker range. Diamonds represent outliers,
223 that is, values outside the whisker range. (C) Histogram of the thirty average
224 spontaneous peak frequencies per person, averaged over the four experimental days.
225 (D) Scatter plot showing the correlation between the total performance accuracy and
226 the spontaneous peak frequency, both averaged over experimental days.

227 *3.2. The power at the individual resting-state peak frequency is not associated with*
228 *the language performance*

229 Second, we examined the relationship between the power at the individual
230 peak frequency during rest (average across four days) and the total performance
231 accuracy. The power was also first estimated for each subject on each day (Fig. 2A)
232 and then averaged across the four days (Fig. 2C). There were no detectable power
233 differences between the four experimental days (Friedman's test $Q = 3.0$, $p = 0.39$;
234 Fig. 2B). We found no clear association between the (average) power and the
235 performance accuracy (Spearman's correlation, $r = -0.09$, $p = 0.64$; Fig. 2D).

236



237

238

239 Figure 2. Relationship between the power of individual spontaneous peak frequency
240 during rest and language task performance. (A) Histogram of the spontaneous peak
241 frequency power of the thirty participants for all four experimental days (120 values).
242 (B) Boxplot of participants' individual spontaneous peak frequency power for each
243 training day (for details, refer to Fig. 1). (C) Histogram of the spontaneous peak
244 frequency power of the thirty participants, averaged over the four experimental days.
245 (D) Scatter plot showing the correlation over participants between the total

246 performance accuracy and the average spontaneous peak frequency power. Total
247 performance accuracy was calculated by averaging the accuracy scores of the four
248 experimental days, including, both, double and single embedded sentences. Average
249 spontaneous peak frequency powers were averaged over experimental days (shown in
250 C).

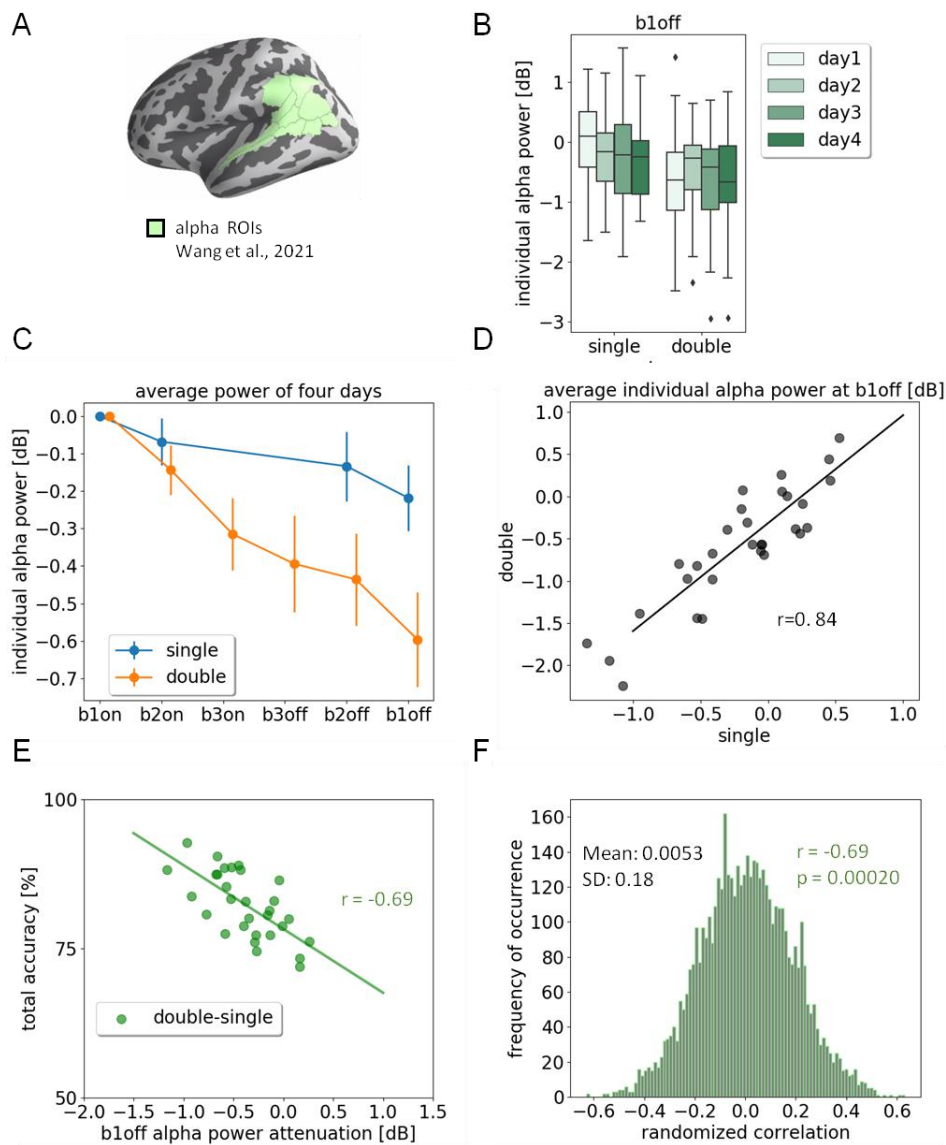
251 3.3. The power at the individual resting-state peak frequency during task was 252 associated with the language performance

253 After examining the individual peak frequency and its power at rest, we
254 examined the power at the same individual frequencies when participants were
255 hearing the sentences, and tested its relationship with the language task performance
256 at single subject level. We expected that the *difference* in power attenuation between
257 the double embedded and single embedded sentences would reflect the subjects'
258 ability to process the sentences. To test this hypothesis, we focused on the brain
259 regions (Fig. 3A), for which in our previous study (Wang et al., 2021) we found a
260 significant difference in the alpha power (8-12 Hz) attenuation between the double
261 and single embedding conditions at the final closure of the embedding structure (*bloff*;
262 Fig. S5; for the meaning of the trigger point labels *b1on*, *b1off*, *b2on*, *b2off*, see
263 Materials and Methods section 2.2.). We first examined, whether by using the
264 individual resting-state peak frequency, we can replicate our previous result obtained
265 with the broad alpha band (sentence effect: general power attenuation difference
266 between double and single embedded sentences). In Fig. 3B we show the power
267 decrease at the individual peak frequency at *bloff* (*bloff-b1on*) for each sentence type
268 and each day. A non-parametric ANOVA (Wobbrock et al., 2011) for the factors
269 sentence (double vs. single) and day (1 through 4) revealed only a significant main
270 effect for the factor sentence ($F = 26.10$, $p = 7.44E-7$). Averaged across all four days,
271 for both types of sentences, the alpha power decreases when sentence unfolds. The
272 difference between the power attenuation between sentence types increased over the
273 sentence and was most pronounced at *bloff* (Fig. 3C). The power attenuations at *bloff*
274 for single and double embedded sentences were strongly correlated (Spearman's
275 correlation $r = 0.84$, $p = 9.00E-9$; Fig. 3D).

276 Most importantly, as hypothesized, at *bloff*, the alpha power attenuation
277 difference between single and double embedded sentences was correlated with the
278 individual task performance (Spearman's correlation $r = -0.64$, $p = 2.63E-5$; Fig. 3E):

279 participants who showed a larger power attenuation difference between the two
280 sentence types at their individual peak frequency achieved better overall accuracy.
281 Moreover, those participants, who showed a larger power attenuation for the double
282 embedded sentences also performed better (Spearman's $r = -0.44$, $p = 0.015$; see
283 supplementary Fig. S1).

284 When using the classical frequency band (8-12 Hz, as reported in (Wang et al.,
285 2021) instead of the individual peak frequency, the by-subject correlation between
286 *bloff* power attenuation difference (double vs. single) and the performance reduced to
287 $r = -0.50$ (Spearman's correlation, $p = 0.0049$), and the correlation between the *bloff*
288 power attenuation for double embedding and the performance dropped to $r = -0.28$
289 (Spearman's correlation, $p = 0.13$; see supplementary Fig. S2).



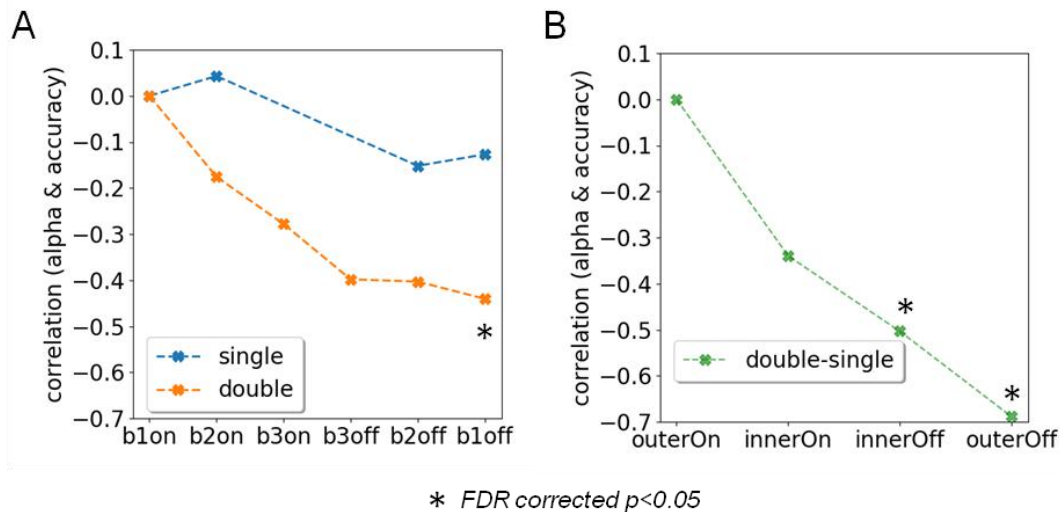
291 Figure 3. Relationship between the power attenuation at individual peak frequency
292 during task and the language task performance. (A) Pre-selected ROIs that were
293 reported to show significant power attenuation difference between double- and single
294 embeddings at the final closure of the embedded structure in Wang et al., 2021. (B)
295 Boxplot of the individual alpha power attenuation for each sentence type and each day.
296 The individual alpha power attenuation was estimated by the power of the individual
297 peak frequency at the final closure of the embedded structure (*bl_{off}*) minus the power
298 at the start of the embedded structure (*bl_{on}*). (C) Four-days-average individual alpha
299 power attenuation for each sentence type at different openings and closures of the
300 embedded structure. Points show the mean value of the thirty participants, vertical
301 lines show the standard error. The power of *bl_{on}* (opening of the embeddings) was
302 used as baseline for the other positions. (D) The individual alpha power attenuations
303 at the final closures (*bl_{off}*) for double and single embedded sentences were strongly
304 associated (Spearman's correlation, $p = 9.00E-9$). (E) The power attenuation
305 differences between double and single embedded sentences at the individual alpha
306 frequency at the final closure were associated with the individual performance
307 accuracy (Spearman's correlation, $p = 2.63E-5$). (F) Permutation-test of the
308 association between the individual alpha power attenuation differences (double vs.
309 single embedded sentence) at the final closure and the individual task performance.
310 The power attenuations of the single as well as the double embedded sentences were
311 permuted 5000 times. The mean of the randomized Spearman's correlation was
312 0.0053 and the standard deviation was 0.18. The probability of appearance of a
313 correlation value that less than $r = -0.69$ was 0.0002.

314

315 *3.4. Temporal exploration: association of alpha power attenuation and language* 316 *performance at different embedding levels*

317 Fig. 4A shows the Spearman's correlation between the total performance accuracy
318 and the individual peak frequency power attenuation (i.e., with respect to *bl_{on}*) for
319 both sentence types at different positions of the embedded structure. Fig. 4B shows, at
320 individual peak frequency, the power attenuation *difference* between the two sentence
321 types at equivalent positions: *innerOn/innerOff* and *outerOn/outerOff*
322 (opening/closure of the innermost/outermost embedded structures). After FDR-
323 correction, we found three significant correlations. In addition to the power

324 attenuation at the final embedding closure for double embedded sentence and the
325 power attenuation difference at the final embedding closure, which were already
326 reported (Fig. 3E, & Fig. S1A), we found a performance correlation with the power
327 attenuation difference at the first embedding closure (*innerOff*; Spearman's $r = -0.50$,
328 FDR $p < 0.05$; Fig. 4B).



329

330 Figure 4. Association of the individual peak frequency power attenuation and the
331 language performance at different positions of embedded structures. (A)
332 Spearman's correlation between the individual peak frequency power attenuation
333 (with respect to baseline b1on) for double and single embedded sentences and the
334 total performance accuracy. (B) Spearman's correlation between the individual peak
335 frequency power attenuation difference (double-single) and the total performance
336 accuracy at different syntactically equivalent position. Position labels: outerOn: b1on
337 for single and double; innerOn: b2on for single and b3on for double; innerOff: b2off
338 for single and b3off for double; outerOff: b1off for single and double.

339

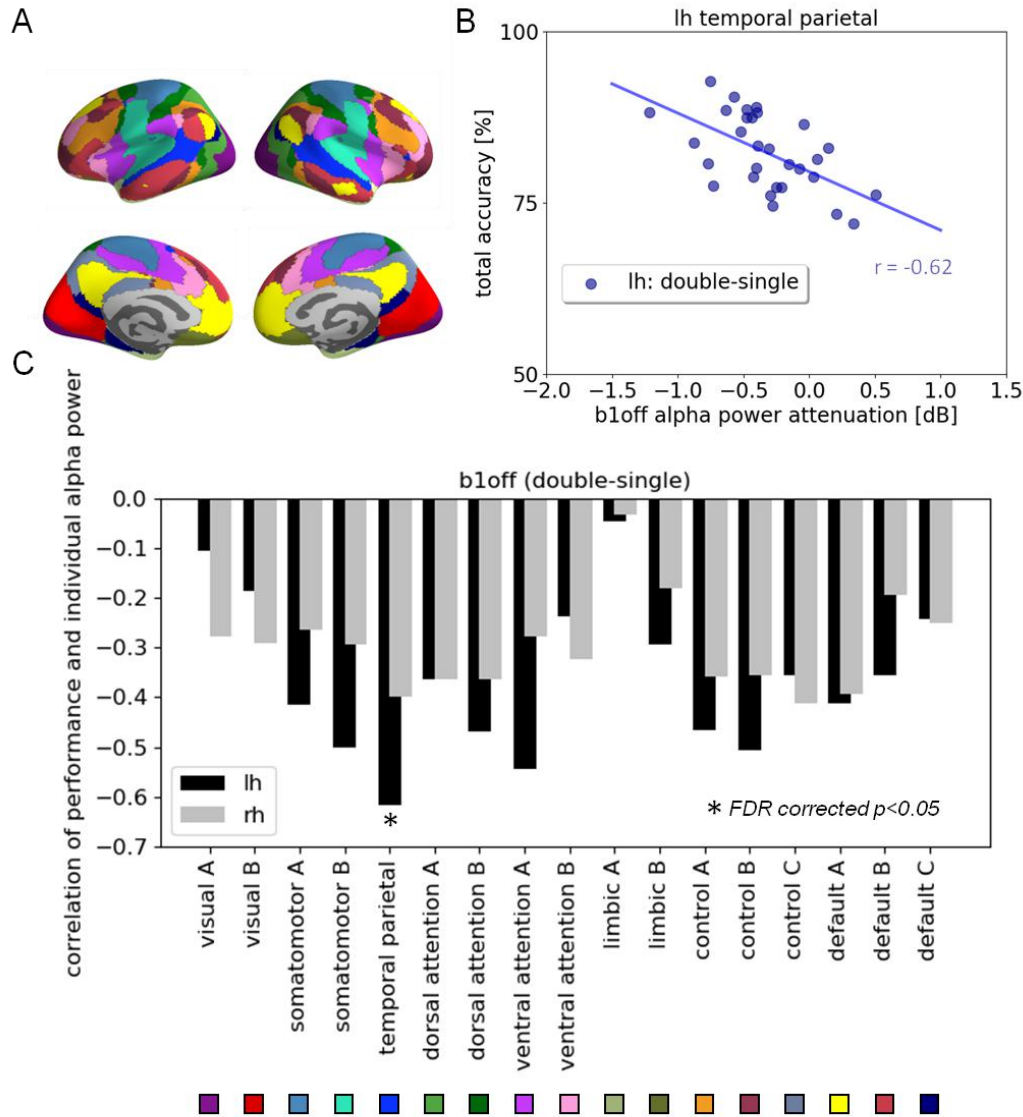
340 3.5. Spatial exploration: association of individual peak frequency power attenuation 341 and language performance at the functional network level

342 We explored the correlation between the individual peak frequency power
343 attenuation and the power attenuation difference (double vs. single embedding) of the
344 individual peak frequency at *b1off* and the total performance at the cortical level. In
345 order to achieve maximum specificity to functional networks, we used the Yeo's 17-
346 networks (Thomas Yeo et al., 2011) to define the brain ROIs (Fig. 5A). The power

347 attenuation difference in the left temporal-parietal network (including the anterior and
348 posterior superior temporal gyrus, Fig. 5A bright blue ROI) was significantly
349 correlated with task performance (Spearman's $r = -0.62$, FDR corrected $p < 0.05$; Fig.
350 5B&C). Also, the power attenuation for double embedded sentence in the right
351 temporal-parietal network (including anterior and posterior superior temporal gyrus,
352 Fig. 5A bright blue ROI) was significantly correlated with the performance
353 (Spearman's $r = -0.62$, FDR corrected $p < 0.05$; Fig. S3B&C).

354 Additional information about the spatial exploration of the correlation between
355 the individual peak frequency power attenuation at the final closure of the embedded
356 structure and the language performance based on the Glasser atlas (Glasser et al.,
357 2016) can be found in Fig. S5. We obtained similar results as for the Yeo's 17-
358 networks: in the left anterior and posterior superior temporal gyri, the power
359 attenuation difference between double and single embedded sentences was correlated
360 with the language performance, while in the right middle and posterior superior
361 temporal gyri, as well as inferior frontal gyrus, the power attenuation for double
362 embedded sentences was correlated with the performance.

363



364

365 Figure 5. Association of the individual peak frequency power attenuation and the
 366 language performance at the functional networks level. (A) ROIs of Yeo's 17-
 367 networks. The temporal parietal network is painted in bright blue. (B) Individual peak
 368 frequency power attenuation difference (double vs. single embeddings) at the final
 369 closure of the embedded structures (*b1off*) in the left temporal-parietal network (lh:
 370 double-single) was significantly associated with the performance (Spearman's $r = -$
 371 0.62, FDR corrected $p < 0.05$). (C) Spatial distribution of the Spearman's correlation
 372 between individual peak frequency power attenuation difference (double vs. single
 373 embeddings) at the final closure of the embedded structures (*b1off*) and the individual
 374 performance accuracy on Yeo's 17-networks.

375

376 **4. Discussion**

377 In this study, we investigated the association between language comprehension
378 performance and individual dominant oscillations under resting-state and in-task
379 conditions. The individual peak frequency, as determined at sensor level at rest, was
380 found in the alpha band for most participants. This individual peak frequency as well
381 as the spectral power at that frequency at rest did not significantly change over the
382 course of the experiment, nor did they correlate with the individual language
383 performance.

384 Next, we turned to the MEG data acquired during task, by studying the
385 spectral power attenuation at the individual peak frequency (as determined at rest).
386 We tested our hypothesis that the individual power attenuation over the course of each
387 sentence predicts the individual language comprehension performance. Indeed, we
388 found correlations for, both, the power attenuation observed for the more complex
389 sentences (double embedding) and the difference in power attenuation between the
390 two complexity levels. While the same effects could be replicated when simply using
391 the entire alpha band (8-12 Hz) instead of the individual peak frequency, the
392 correlations were considerably weaker in that case. Interestingly, a spatial analysis
393 based on a network atlas (Yeo's 17-networks) suggested that the difference between
394 the power attenuations is present in a temporal-parietal network in the left hemisphere,
395 while the effect of the double embedding condition alone localizes in its right
396 hemisphere homologue.

397 Hence, in summary, the following observations underscore the functional role
398 of these individually dominant (mostly alpha band) oscillations in language
399 processing: (i) individual performance was correlated with alpha power attenuation
400 during task but not with alpha power at rest, and (ii) these effects were localized in
401 temporal-parietal brain regions usually associated with language processing.

402 Cortical alpha activity has been proposed to play an important role in
403 excitability regulation mechanisms underlying various human cognitive abilities,
404 including memory, attention, perception, etc. Task irrelevant regions exhibit higher
405 alpha power reflecting inhibition, while in task relevant regions alpha power is
406 reduced, reflecting increased excitability (Foxye & Snyder, 2011; Jensen & Mazaheri,
407 2010; Klimesch, 2012; Klimesch et al., 2007).

408 At rest, such an increased excitability could reflect a general predisposition of
409 a person towards cognitive performance. In contrast, if observed during task within
410 specific task relevant brain areas, it would index processes related to the particular
411 task or experimental situation. Alpha power at rest has been found to be positively
412 correlated with task performance in cognitive control (Mahjoory et al., 2019) and
413 episodic memory (Sargent et al., 2021) tasks, but negatively correlated with language
414 skills (Kwok et al., 2019). This somewhat non-univocal picture suggests that for
415 different experimental situations, different levels of pre-inhibition and disinhibition of
416 cortical areas are beneficial. On the other hand, during the actual task and within the
417 task relevant areas, we would expect a clear attenuation of alpha, which scales with
418 the actual engagement with the task reflected by task performance. There are a
419 number of previous studies showing general alpha attenuation during task within task
420 relevant areas (Hilla et al., 2020; Magosso et al., 2019; Wang et al., 2021). These
421 works show that the alpha oscillation power is related to the specific task demand.
422 This is reflected in our results by the finding that the individual alpha power
423 attenuation is stronger for the more complex sentences and increases with increasing
424 cognitive (including working memory) load along the sentence. On the other hand,
425 evidence for a correlation between alpha power modulation in specific task-relevant
426 brain areas and individual task performance is scarce. By clearly demonstrating this in
427 our study, we show that in-task alpha power attenuation actually reflects processes
428 that are involved in successful task completion.

429 Along with the idea that the association of the alpha power and performance
430 may indicate the task engagement of the brain regions, our results based on Yeo's 17-
431 networks suggest that the temporal-parietal network plays a crucial role in processing
432 the embedding. We further cross-checked and refined this by exploring the
433 association using the whole 360 ROI brain parcellation from the Glasser atlas and
434 found a particularly high association between power attenuation difference (double vs.
435 single) and performance in the superior temporal gyrus (Fig. S4. A). This is in
436 alignment with the literature showing that the posterior superior temporal gyrus plays
437 an important role in processing embedded structures (Friederici, 2011; Friederici et al.,
438 2006; Kinno et al., 2008; Röder et al., 2002). Regarding the differential findings in the
439 two homologue networks in the left and right hemispheres, we infer that even though
440 the areas in the left hemisphere form the classical language network (Friederici, 2011;
441 Hickok & Poeppel, 2004; Poeppel et al., 2012; Vigneau et al., 2006), homologue

442 areas in the right hemisphere may increasingly engage when task demands are high as
443 a result of enhanced working memory loads (Fridriksson & Morrow, 2005). This
444 would explain why we find right hemispheric effects for the double embedded
445 sentences, but not for the single embedded ones. Nevertheless, this notion alone
446 would predict effects for both embedding levels in the left hemisphere as well. Instead,
447 we only found an effect of the difference between these two levels, that is, on how
448 much the alpha power attenuation increases when the task complexity rises. How
449 could that be accounted for? One possible explanation is the following. Normal
450 language processing only engages the left hemisphere language areas and leads there
451 to an alpha power attenuation over the course of the sentence, which is strongly
452 individually specific. Some persons have a large attenuation and others a smaller one,
453 irrespective of the presented material. This causes a strong correlation between the
454 alpha power attenuation between single and double embedded sentences (Fig. 3D).
455 Then, there is an additional alpha power attenuation that is related to the cortical
456 engagement with the task, and hence to sentence complexity (Fig. 3C) and task
457 performance (Fig. 3E). While for each single condition (single and double embedding,
458 respectively) this correlation is obscured by the large inter-individual fluctuation, in
459 the difference between the two conditions this influence is cancelled out and the
460 correlation with performance becomes significant. The right hemisphere areas, in
461 contrast, are not so much involved in normal language processing and only step in to
462 cope with the high task demand in the double embedding condition. Therefore, the
463 alpha power attenuation is mainly task related and hence correlates with the task
464 performance.

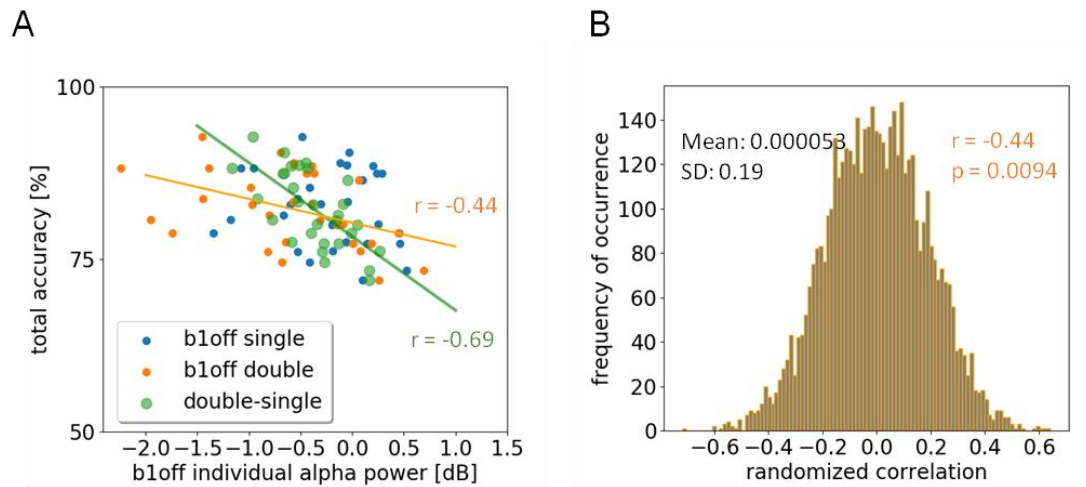
465

466 **5. Conclusion**

467 In summary, in this present paper, we used a language comprehension
468 experiment to demonstrate that by manipulation of the task complexity, the alpha
469 power attenuation in the task relevant brain regions, especially the individual alpha,
470 reflect the increase of the cognitive load and predicted the individual performance
471 outcome. Individual alpha power could be a useful biomarker to highlight the relevant
472 brain regions and monitor the brain states during the cognitive processing.

473

474 **6. Supplementary Figures**

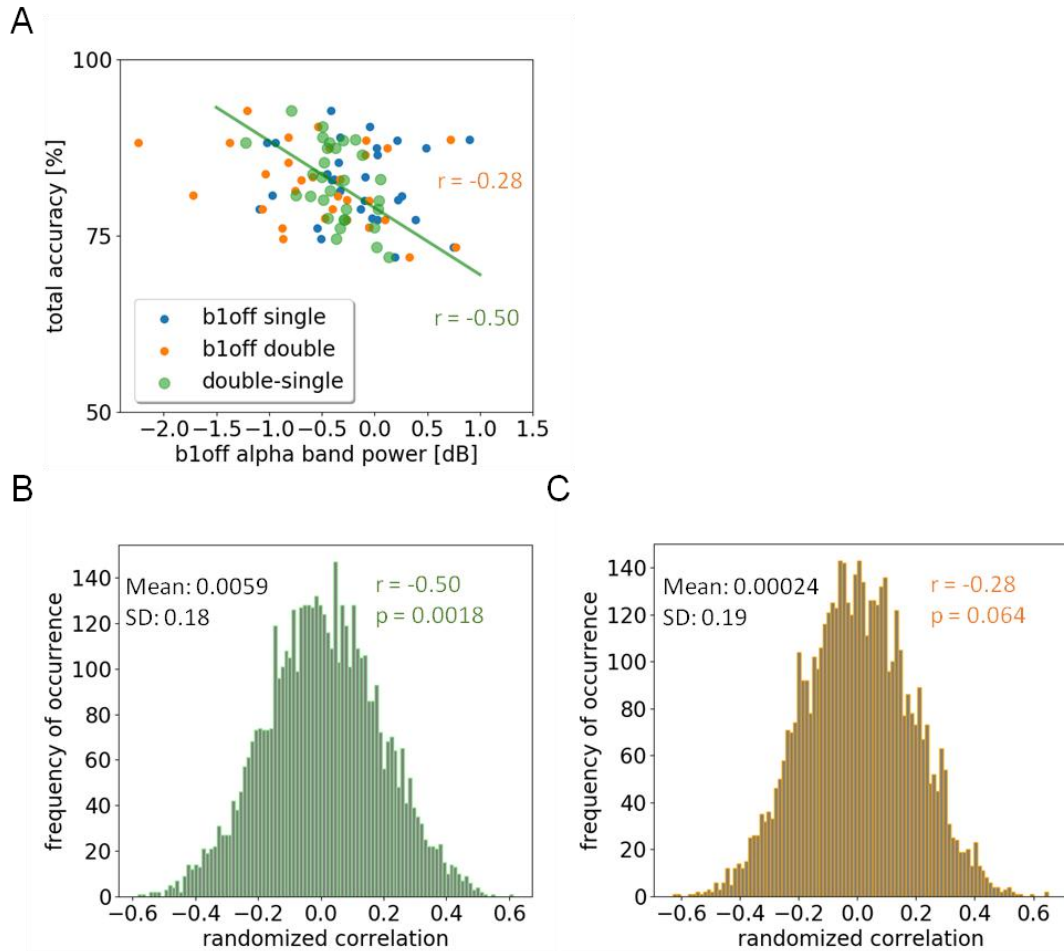


476 Figure S1. Association between the individual peak frequency power attenuation at
477 the final closure of the embedded structure (*b1off*) and the total performance accuracy.
478 (A) Individual peak frequency power attenuation for double embedded sentences was
479 associated with the performance accuracy (Spearman's $r = -0.44$, $p = 0.015$). (B)
480 Permutation-test of the association between the individual peak frequency power
481 attenuation (*b1off*) for double embedded sentences and the performance accuracy. The
482 power attenuation values were permuted for 5000 times. The mean of the randomized
483 Spearman's correlation was 0.00 and the standard deviation was 0.19. The probability
484 of appearance of a correlation value less than $r = -0.44$ was 0.0094.

485

486

487



488

489 Figure S2. Association between the broad band alpha (8-12 Hz) power attenuation at
490 the final closure of the embedded structure (*b1off*) and the total performance accuracy.

491 (A) Broad band alpha power attenuation difference (double vs. single embeddings)
492 associated with the total performance accuracy (Spearman's $r = -0.50$, $p = 0.0049$). (B)

493 Permutation-test of the association between the broad band alpha power attenuation
494 difference (double vs. single embedded sentence) at the final closure of the

495 embeddings and the individual task performance. The power attenuations of the single
496 as well as the double embedded sentences were permuted for 5000 times. The mean

497 of the randomized Spearman's correlation was 0.0059 and the standard deviation was
498 0.18. The probability of appearance of a correlation value less than $r = -0.50$ was

499 0.0018. (C) Permutation-test of the association between the broad band alpha power
500 attenuation (*b1off*) for double embedded sentences and the performance accuracy. The

501 power attenuations were permuted for 5000 times. The mean of the randomized
502 Spearman's correlation was 0.00024 and the standard deviation was 0.19. The

503 probability of appearance of a correlation value less than $r = -0.28$ was 0.064.

504

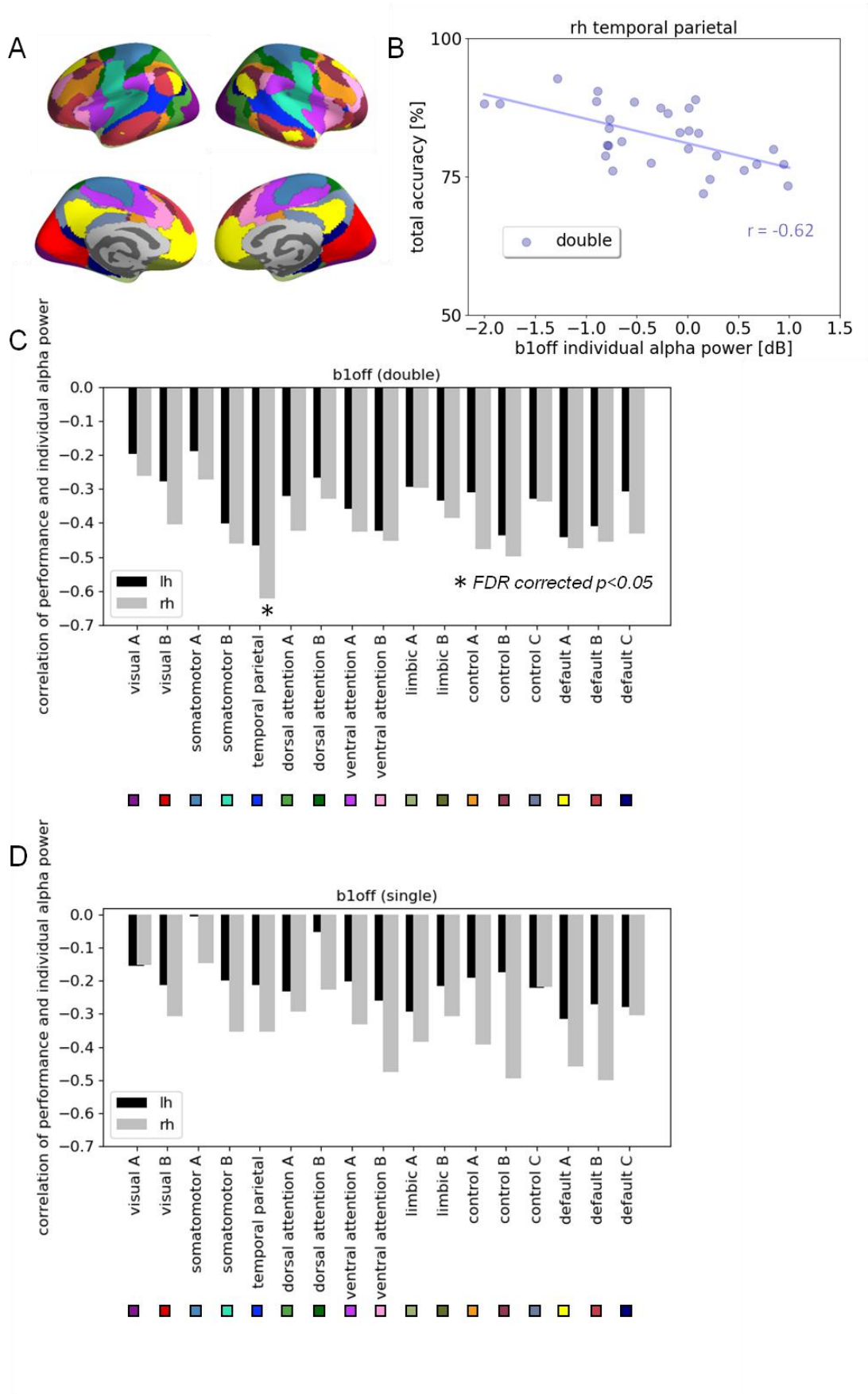
505

506

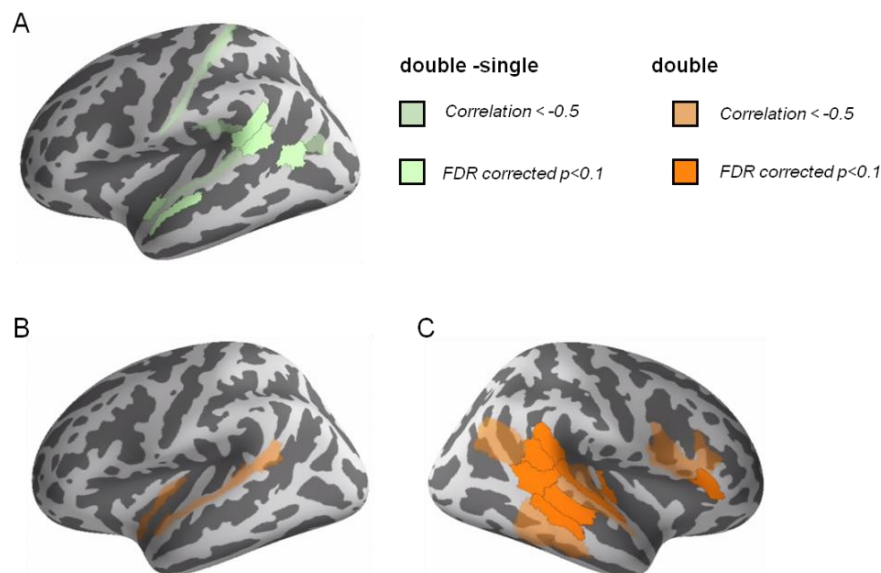
507

508

509



511 Figure S3. Association of the individual peak frequency power attenuation and the
512 language performance at the functional networks. (A) ROIs of Yeo's 17-networks.
513 Temporal parietal networks are marked with bright blue. (B) Individual peak
514 frequency power attenuation for double embedded sentences at the final closure of the
515 embedded structures (*bl*off) on the right temporal-parietal network was significantly
516 associated with the performance (Spearman's $r = -0.62$, FDR corrected $p < 0.05$)
517 (C)&(D) Spatial distribution of the Spearman's correlation between individual peak
518 frequency power attenuation of double (C) and single (D) embedded sentences at the
519 final closure of the embedded structures (*bl*off) and the individual performance
520 accuracy on Yeo's 17-networks.
521
522



523
524

525 Figure S4. Association of the peak frequency power attenuation and the language
526 performance with the Glasser atlas. Spearman's correlation were calculated between
527 the total performance accuracy and the (i) power attenuation difference (double vs.
528 single embeddings) at the final closure of the embedded structure (*bl*off) as well as
529 the power attenuation at the final closure for (ii) double and (iii) single embedded
530 sentences for 360 ROIs. FDR-correction was based on all 1080 tests. Significant level
531 is $p < 0.1$ (A) ROIs that showed the association between power attenuation difference
532 (double vs. Single embeddings) and the total performance accuracy. (B)&(C) ROIs
533 that showed the association between power attenuation for double embedded
534 sentences and the total performance accuracy.

535

536


A. **Anke denkt nicht, dass Malte, der niemals ehrgeizig war, viele Muskeln hat.**


b1on b2on b2off b1off

Anke does not think that Malte, who was never ambitious, has many muscles.

Q: Hat Anke viele Muskeln? / Does Anke have many muscles?

B. **Es war ihr klar, dass Henri, der Betty, die den Jungen adoptierte, fasziniert, glücklich ist.**


b1on b2on b3on b3off b2off b1off

It was clear to her that Henri, who fascinates Betty, who adopted the boy, is happy.

Q: Es war Betty, die Henri fasziniert, oder? / It was Betty who fascinated Henri, wasn't it?

537

538

539

540 Figure S5. Examples of presented sentences in German with English translations in
541 italics: (A) single; (B) double center embedding. We used the data segment starting at
542 *b1on* as a reference to compute the relative alpha power attenuation for all other
543 marked time points. The marker *b1on* represented the beginning of the relative clause
544 containing all hierarchical embedding. Q: Probing questions for the presented
545 examples.

546

547

548

549

550

551

552

553

554

555

556

557

558

559

560

561

562

563

564 7. References

565

566 Berger, H. (1938). Über das Elektrenkephalogramm des Menschen. XIV. *Archiv Für Psychiatrie Und*
567 *Nervenkrankheiten*.

568 Foxe, J. J., & Snyder, A. C. (2011). The role of alpha-band brain oscillations as a sensory suppression
569 mechanism during selective attention. *Frontiers in Psychology*, 2(JUL), 1–13.

570 <https://doi.org/10.3389/fpsyg.2011.00154>

571 Fridriksson, J., & Morrow, L. (2005). Cortical activation and language task difficulty in aphasia.

572 *Aphasiology*, 19(3–5), 239–250.

573 Friederici, A. D. (2011). The brain basis of language processing: from structure to function.

574 *Physiological Reviews*, 91(4), 1357–1392.

575 Friederici, A. D., Bahlmann, J., Heim, S., Schubotz, R. I., & Anwander, A. (2006). The brain

576 differentiates human and non-human grammars: Functional localization and structural

577 connectivity. *Proceedings of the National Academy of Sciences of the United States of America*,

578 103(7), 2458–2463. <https://doi.org/10.1073/pnas.0509389103>

579 Furman, A. J., Meeker, T. J., Rietschel, J. C., Yoo, S., Muthulingam, J., Prokhorenko, M., Keaser, M. L.,

580 Goodman, R. N., Mazaheri, A., & Seminowicz, D. A. (2018). Cerebral peak alpha frequency

581 predicts individual differences in pain sensitivity. *NeuroImage*, 167, 203–210.

582 Gastaldon, S., Arcara, G., Navarrete, E., & Peressotti, F. (2020). Commonalities in alpha and beta

583 neural desynchronizations during prediction in language comprehension and production. *Cortex*,

584 133, 328–345. <https://doi.org/10.1016/j.cortex.2020.09.026>

585 Glasser, M. F., Coalson, T. S., Robinson, E. C., Hacker, C. D., Harwell, J., Yacoub, E., Ugurbil, K.,

586 Andersson, J., Beckmann, C. F., & Jenkinson, M. (2016). A multi-modal parcellation of human

587 cerebral cortex. *Nature*, 536(7615), 171–178.

588 Grabot, L., & Kayser, C. (2020). Alpha activity reflects the magnitude of an individual bias in human

589 perception. *Journal of Neuroscience*, 40(17), 3443–3454.

590 Gramfort, A., Luessi, M., Larson, E., Engemann, D. A., Strohmeier, D., Brodbeck, C., Goj, R., Jas, M.,

591 Brooks, T., & Parkkonen, L. (2013). MEG and EEG data analysis with MNE-Python. *Frontiers in*

592 *Neuroscience*, 7, 267.

593 Gulbinaite, R., van Viegen, T., Wieling, M., Cohen, M. X., & VanRullen, R. (2017). Individual alpha peak

594 frequency predicts 10 Hz flicker effects on selective attention. *Journal of Neuroscience*, 37(42),

595 10173–10184.

596 Hickok, G., & Poeppel, D. (2004). Dorsal and ventral streams: a framework for understanding aspects

597 of the functional anatomy of language. *Cognition*, 92(1–2), 67–99.

598 Hilla, Y., von Mankowski, J., Föcker, J., & Sauseng, P. (2020). Faster Visual Information Processing in

599 Video Gamers Is Associated With EEG Alpha Amplitude Modulation. *Frontiers in Psychology*, 11,

600 3333.

- 601 Horschig, J. M., Jensen, O., van Schouwenburg, M. R., Cools, R., & Bonnefond, M. (2014). Alpha
602 activity reflects individual abilities to adapt to the environment. *NeuroImage*, *89*, 235–243.
- 603 Jensen, O., & Mazaheri, A. (2010). Shaping functional architecture by oscillatory alpha activity: gating
604 by inhibition. *Frontiers in Human Neuroscience*, *4*, 186.
- 605 Jones, S. R., Kerr, C. E., Wan, Q., Pritchett, D. L., Hämäläinen, M., & Moore, C. I. (2010). Cued spatial
606 attention drives functionally relevant modulation of the mu rhythm in primary somatosensory
607 cortex. *Journal of Neuroscience*, *30*(41), 13760–13765.
- 608 Katyal, S., He, S., He, B., & Engel, S. A. (2019). Frequency of alpha oscillation predicts individual
609 differences in perceptual stability during binocular rivalry. *Human Brain Mapping*, *40*(8), 2422–
610 2433.
- 611 Kinno, R., Kawamura, M., Shioda, S., & Sakai, K. L. (2008). Neural correlates of noncanonical syntactic
612 processing revealed by a picture-sentence matching task. *Human Brain Mapping*, *29*(9), 1015–
613 1027.
- 614 Klimesch, W. (2012). Alpha-band oscillations, attention, and controlled access to stored information.
615 *Trends in Cognitive Sciences*, *16*(12), 606–617. <https://doi.org/10.1016/j.tics.2012.10.007>
- 616 Klimesch, W., Pfurtscheller, G., Mohl, W., & Schimke, H. (1990). Event-related desynchronization,
617 ERD-mapping and hemispheric differences for words and numbers. *International Journal of*
618 *Psychophysiology*, *8*(3), 297–308.
- 619 Klimesch, W., Sauseng, P., & Hanslmayr, S. (2007). EEG alpha oscillations: the inhibition–timing
620 hypothesis. *Brain Research Reviews*, *53*(1), 63–88.
- 621 Kwok, E. Y. L., Cardy, J. O., Allman, B. L., Allen, P., & Herrmann, B. (2019). Dynamics of spontaneous
622 alpha activity correlate with language ability in young children. *Behavioural Brain Research*, *359*,
623 56–65. <https://doi.org/10.1016/j.bbr.2018.10.024>
- 624 Magosso, E., De Crescenzo, F., Ricci, G., Piastra, S., & Ursino, M. (2019). EEG alpha power is
625 modulated by attentional changes during cognitive tasks and virtual reality immersion.
626 *Computational Intelligence and Neuroscience*, *2019*. <https://doi.org/10.1155/2019/7051079>
- 627 Mahjoory, K., Cesnaite, E., Hohlefeld, F. U., Villringer, A., & Nikulin, V. V. (2019). Power and temporal
628 dynamics of alpha oscillations at rest differentiate cognitive performance involving sustained
629 and phasic cognitive control. *Neuroimage*, *188*, 135–144.
- 630 Mann, C. A., Sterman, M. B., & Kaiser, D. A. (1996). Suppression of EEG rhythmic frequencies during
631 somato-motor and visuo-motor behavior. *International Journal of Psychophysiology*, *23*(1–2), 1–
632 7.
- 633 Migliorati, D., Zappasodi, F., Perrucci, M. G., Donno, B., Northoff, G., Romei, V., & Costantini, M.
634 (2020). Individual alpha frequency predicts perceived visuotactile simultaneity. *Journal of*
635 *Cognitive Neuroscience*, *32*(1), 1–11.
- 636 Minami, S., Oishi, H., Takemura, H., & Amano, K. (2020). Inter-individual differences in occipital alpha
637 oscillations correlate with white matter tissue properties of the optic radiation. *Eneuro*, *7*(2).
- 638 Pfurtscheller, G. (1989). Functional Topography During Sensorimotor Activation Studied with Event-

- 639 Related Desynchronization Mapping. *Journal of Clinical Neurophysiology*, 6(1), 75–84.
640 <https://doi.org/10.1097/00004691-198901000-00003>
- 641 Pfurtscheller, G. (2003). Induced Oscillations in the Alpha Band: Functional Meaning. *Epilepsia*, 44(12
642 SUPPL.), 2–8. <https://doi.org/10.1111/j.0013-9580.2003.12001.x>
- 643 Poeppel, D., Emmorey, K., Hickok, G., & Pylkkänen, L. (2012). Towards a new neurobiology of
644 language. *Journal of Neuroscience*, 32(41), 14125–14131.
- 645 Rathee, S., Bhatia, D., Punia, V., & Singh, R. (2020). Peak Alpha Frequency in Relation to Cognitive
646 Performance. *Journal of Neurosciences in Rural Practice*, 11(3), 416–419.
647 <https://doi.org/10.1055/s-0040-1712585>
- 648 Röder, B., Stock, O., Neville, H., Bien, S., & Rösler, F. (2002). Brain activation modulated by the
649 comprehension of normal and pseudo-word sentences of different processing demands: a
650 functional magnetic resonance imaging study. *Neuroimage*, 15(4), 1003–1014.
- 651 Sadaghiani, S., & Kleinschmidt, A. (2016). Brain networks and α -oscillations: structural and functional
652 foundations of cognitive control. *Trends in Cognitive Sciences*, 20(11), 805–817.
- 653 Sargent, K., Chavez-Baldini, U., Master, S. L., Verweij, K. J. H., Lok, A., Sutterland, A. L., Vulink, N. C.,
654 Denys, D., Smit, D. J. A., & Nieman, D. H. (2021). Resting-state brain oscillations predict cognitive
655 function in psychiatric disorders: A transdiagnostic machine learning approach. *NeuroImage:*
656 *Clinical*, 30, 102617.
- 657 Schomer, D. L., & Da Silva, F. L. (2012). *Niedermeyer's electroencephalography: basic principles,*
658 *clinical applications, and related fields*. Lippincott Williams & Wilkins.
- 659 Sklar, B., Hanley, J., & Simmons, W. W. (1972). An EEG experiment aimed toward identifying dyslexic
660 children. *Nature*, 240(5381), 414–416.
- 661 Smit, C. M., Wright, M. J., Hansell, N. K., Geffen, G. M., & Martin, N. G. (2006). Genetic variation of
662 individual alpha frequency (IAF) and alpha power in a large adolescent twin sample.
663 *International Journal of Psychophysiology*, 61(2), 235–243.
- 664 Thomas Yeo, B. T., Krienen, F. M., Sepulcre, J., Sabuncu, M. R., Lashkari, D., Hollinshead, M., Roffman,
665 J. L., Smoller, J. W., Zöllei, L., & Polimeni, J. R. (2011). The organization of the human cerebral
666 cortex estimated by intrinsic functional connectivity. *Journal of Neurophysiology*, 106(3), 1125–
667 1165.
- 668 Van Dijk, H., Schoffelen, J.-M., Oostenveld, R., & Jensen, O. (2008). Prestimulus oscillatory activity in
669 the alpha band predicts visual discrimination ability. *Journal of Neuroscience*, 28(8), 1816–1823.
- 670 van Ede, F., Köster, M., & Maris, E. (2012). Beyond establishing involvement: quantifying the
671 contribution of anticipatory α - and β -band suppression to perceptual improvement with
672 attention. *Journal of Neurophysiology*, 108(9), 2352–2362.
- 673 Van Veen, B. D., Van Drongelen, W., Yuchtman, M., & Suzuki, A. (1997). Localization of brain electrical
674 activity via linearly constrained minimum variance spatial filtering. *IEEE Transactions on*
675 *Biomedical Engineering*, 44(9), 867–880.
- 676 Vigneau, M., Beaucousin, V., Hervé, P.-Y., Duffau, H., Crivello, F., Houde, O., Mazoyer, B., & Tzourio-

- 677 Mazoyer, N. (2006). Meta-analyzing left hemisphere language areas: phonology, semantics, and
678 sentence processing. *Neuroimage*, 30(4), 1414–1432.
- 679 Wang, P., Knösche, T. R., Friederici, A. D., Maess, B., Chen, L., & Brauer, J. (2021). Functional brain
680 plasticity during L1 training on complex sentences : Changes in gamma-band oscillatory activity.
681 *Human Brain Mapping*, March, 1–13. <https://doi.org/10.1002/hbm.25470>
- 682 Wobbrock, J. O., Findlater, L., Gergle, D., & Higgins, J. J. (2011). The aligned rank transform for
683 nonparametric factorial analyses using only anova procedures. *Proceedings of the SIGCHI*
684 *Conference on Human Factors in Computing Systems*, 143–146.
- 685